AIAA 80-1102R

Shuttle Subscale Ablative Nozzle Tests

L.B. Powers*
NASA Marshall Space Flight Center,
and
R.L. Bailey†
Jet Propulsion Laboratory, California Institute of Technology, Pasadena, Calif.

Recent subscale nozzle tests have identified new and promising carbon phenolic ablatives which utilize staple rayon, polyacrylonitrile, and pitch based carbon cloth. A 4-in. throat diameter submerged test nozzle, designed for the 48-in. Jet Propulsion Laboratory char motor, was used to evaluate five different designs incorporating 20 candidate ablatives. A 3200 lb Shuttle solid rocket motor polybutadiene acrylic acid acrylonitrile propellant grain provided a chamber pressure-burn time environment similar to the first 45 s of the Shuttle solid rocket motor.

Introduction

SEVERAL new and promising ablative materials have recently been introduced. Limited subscale solid rocket nozzle tests have indicated that staple rayon, polyacrylonitrile (PAN) in staple and continuous form, and continuous pitch based materials are prime candidates for use in nozzle ablative liners. Staple rayon fiber is used in large quantities in commercial products and availability appears assured because of large commercial demand, multiple domestic producers, and projected cost stability. Pitch is an attractive carbon fiber precursor due to low energy conversion requirements, high carbon content, high carbonization yield, and low price. PAN fibers also have high carbon content, low cost, and a large relatively stable market.

The solid rocket motor (SRM) nozzle requires approximately 12,500 lb of carbon fabric reinforced prepreg ablative tape to wrap the ablative liner components. A lower cost ablative, or one which offers improved erosion and char performance, could substantially reduce the cost of the SRM nozzle. The nozzle test program was initiated to evaluate these new ablative materials for potential application in this nozzle. The objective of the program was to test the candidate ablative materials, as supplied by the vendors, in an SRM environment. Complete characterization of these new ablatives was beyond the scope of the program.

The following sections of this article discuss the details of the test motor and nozzle configuration and present the results from the post-test analyses.

Test Configuration, Nozzle

Figure 1 is a cross-sectional view of the test nozzle designed to simulate the Shuttle SRM nozzle in a subscale mode without thrust vector control (TVC). The test nozzle initial throat diameter is 4.0 in. and the initial expansion ratio is 8:1. Ablative liner components are supported by a 4130 steel shell. In order to maximize the erosion and char performance data from each test, the nozzle nose ring, the throat ring, and the exit cone were fabricated using two ablatives in a split ring-type construction. These are shown in Fig. 2 with numbers assigned to the ablative components. Figure 2 also lists the construction methods employed to fabricate each component.

A total of six nozzles were fabricated and Tables 1-4 list the location of the candidate materials selected for each nozzle. Also listed are the precursor, form (carbon or graphite), fabric, weave, final specific gravity, and manufacturer. Nose and throat rings were fabricated by the stacked laminate method and cured as one part. An alternating 15-deg overlap was used in the stacking process at the interface of the two ablatives to minimize any localized discontinuities. In the case of the exit cone, two exit cone liners were tapewrapped and then sectioned into two equal parts. Finally, one side from each part was assembled on a mandrel and cured as one part. Component 4, the nozzle backside ring, consisted of one material and was tapewrapped and cured on the steel support shell. Component 5, the backside insulation, was fabricated

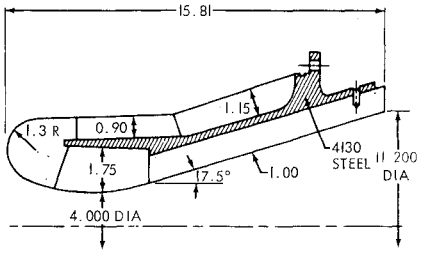

NOTE: ALL DIMENSIONS ARE IN INCHES.

Fig. 1 Test nozzle cross-sectional view.

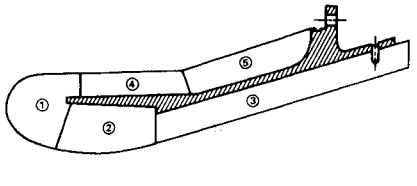

- COMPONENTS 1,2, AND 3 CONSIST OF TWO MATERIALS EACH.
- COMPONENTS 1 AND 2 ARE FABRICATED BY THE STACKED LAMINATE METHOD AND CURED AS ONE PART.
- COMPONENT 3 IS A TAPEWRAPPED SPLIT RING OF TWO MATERIALS CURED TOGETHER
- COMPONENT 4 IS ONE MATERIAL TAPEWRAPPED AND CURED ON THE SHELL.
- COMPONENT 5 IS FABRICATED BY THE HAND LAY-UP METHOD AND CURED ON THE SHELL.

Fig. 2 Nozzle general arrangement and component fabrication methods.

Presented as Paper 80-1102 at the AIAA/SAE/ASME 16th Joint Propulsion Conference, Hartford, Conn., June 30-July 2, 1980; submitted July 24, 1980; revision received July 22, 1981. This paper is declared a work of the U.S. Government and therefore is in the public domain.

*Member of Technical Staff, Solid Motors Branch.
†Supervisor, Solid Propulsion Technology Group. Member AIAA.

Table 1 Nose cap components

Nozzle S/N	Section	Material code[a]	Fabric	Weave	Fabric supplier	Precursor (resin no.)	Type	Final S.G.
SAA-1	A	FM5749	VCB-20	8HS	Union Carbide	Continuous pitch (F014)	Carbon	1.63
	B	FM5748	Hitex P-223	8HS	HITCO Structures	Staple PAN (F014)	Carbon	1.51
SAA-2	A	K408P	VCB-20	8HS	Union Carbide	Continuous pitch (HT-494C)	Graphite	1.65
	B	K411	SWB-8	8HS	Stackpole	Staple PAN (HT-494C)	Graphite	1.55
SAA-3	A	K418	VCB-45	8HS	Union Carbide	Continuous pitch (HT-494C)	Graphite	1.63
	B	K414	PWB-6	Plain	Stackpole	Staple PAN (HT-494C)	Graphite	1.58
SAA-4	A	MX4940	CSA-5	8HS	Polycarbon	Staple rayon (HT-428A)	Carbon	1.50
	B	MX4926[b]	CSA	8HS	Polycarbon	Continuous rayon (HT-428A)	Carbon	1.47
SAA-5	A[c]	FM5878	T-300	Plain	Union Carbide	Continuous PAN (F014)	Carbon	1.60
SAA-6	A	FM5750	VCB-45	8HS	Union Carbide	Continuous pitch (F014)	Graphite	1.47
	B	FM5064	WCA	Plain	Union Carbide	Continuous rayon (F064)	Graphite	1.68

[a]For Tables 1-4, FM is a U.S. Polymeric, Inc. material code; K and MX are Fiberite, Corp. material codes. [b]This is a Shuttle qualified baseline nozzle ablative material. [c]The nose cap for SAA-5 was a continuous ring of material.

Table 2 Throat components

Nozzle S/N	Section	Material code	Fabric	Weave	Fabric supplier	Precursor (resin no.)	Type	Final S.G.
SAA-1	A	FM5749	VCB-20	8HS	Union Carbide	Continuous pitch (F014)	Carbon	1.61
	B	FM5748	Hitex P-223	8HS	HITCO Structures	Staple PAN (F014)	Carbon	1.51
SAA-2	A	K408P	VCB-20	8HS	Union Carbide	Continuous pitch (HT-494C)	Graphite	1.68
	B	K411	SWB-8	8HS	Stackpole	Staple PAN (HT-494C)	Graphite	1.55
SAA-3	A	K418	VCB-45	8HS	Union Carbide	Continuous pitch (HT-494C)	Graphite	1.67
	B	K414	PWB-6	Plain	Stackpole	Staple PAN (HT-494C)	Graphite	1.58
SAA-4	A	MX4964	VCC-20	8HS	Union Carbide	Continuous pitch-thin (HT-428A)	Carbon	1.61
	B	MX4960	W-182	8HS	Fiberite	Continuous PAN (HT-428A)	Graphite	1.55
SAA-5	A	MX4964	VCC-20	8HS	Union Carbide	Continuous pitch, thin weave (HT-428A)	Carbon	1.61
	B	FM5878	T-300	Plain	Union Carbide	Continuous PAN (F014)	Carbon	1.60
SAA-6	A	FM5750	VCB-45	8HS	Union Carbide	Continuous pitch (F014)	Graphite	1.72
	B	FM5857	Hi-carbon P-345	8HS	HITCO Structures	Staple PAN (P014)	Graphite	1.56

Table 3 Exit cone components

Nozzle S/N	Section	Material Code	Fabric	Weave	Fabric Supplier	Precursor (resin no.)	Type	Final S.G.
SAA-1	A	FM5055[a]	CCA-3	8HS	HITCO Materials	Continuous rayon (F014)	Carbon	1.48
	B	FM5829	CCA-28	8HS	HITCO Materials	Staple rayon (F014)	Carbon	1.47
SAA-2	A	MX4940	CCA-28	8HS	HITCO Materials	Staple rayon (HT-428A)	Carbon	1.49
	B	K421	KFB	Knit	Stackpole	Staple PAN (HT-494C)	Graphite	1.55
SAA-3	A	K425	HTC-4	8HS	Hercules	Staple PAN (HT-494C)	Graphite	1.54
	B	MX4940	CSA-5	8HS	Polycarbon	Staple rayon (HT-494C)	Carbon	1.45
SAA-4	A	K425	HTC-4	8HS	Hercules	Staple PAN (HT-494C)	Graphite	1.54
	B	K430	VC-0210	8HS	Union Carbide	Staple PAN (HT-494C)	Graphite	1.52
SAA-5	A	MX4960	W-182	8HS	Fiberite	Continuous PAN (HT-494C)	Graphite	1.55
	B	MX4961	W-133	8HS	Fiberite	Continuous PAN (R-113, unfilled)	Graphite	1.52
SAA-6	A	FM5855	G-2206	8HS	HITCO Materials	Continuous rayon (F014)	Graphite	1.39
	B	FM5746	G-2252	8HS	HITCO Materials	Staple rayon (F014)	Graphite	1.47

[a]This is a Shuttle qualified baseline nozzle ablative material.

Table 4 Insulation components

Nozzle S/N	Section[a]	Material Code	Fabric	Weave	Supplier	Material	Type	Final S.G.
SAA-1	A	FM5829	CCA-28	8HS	HITCO Materials	Staple rayon (F014 resin)	Carbon	1.47
	B	JPL-HTPB rubber	None	--	--	Rubber/phenolic microballoons	Elastomer	0.63
SAA-2	A	MX4961	W-133	8HS	Fiberite	Continuous PAN (R-113 resin unfilled)	Graphite	1.52
	B	Flexwrap 1046B	F-1065	Random filled	Fiberite	EPDM rubber/pitch fibers	Filled elastomer	1.10
SAA-3	A	K432	G-2252	8HS	HITCO Materials	Staple rayon (HT-494C resin)	Graphite	1.44
	B	Flexwrap 1061B	F-1065	Random filled	Fiberite	SBR rubber/pitch fibers	Filled elastomer	1.26
SAA-4	A	MX4960	W-182	8HS	Fiberite	Continuous PAN (HT-428A resin)	Graphite	1.55
	B	Flexwrap 1060B	F-1065	Random filled	Fiberite	SBR rubber/pitch fiber	Filled elastomer	1.23
SAA-5	A	FM5856	P-234 lo-carbon	8HS	HITCO Structures	Staple PAN (F014 resin)	Carbon	1.64
	B	2066P	--	--	U.S. Polymeric, Inc.	EPDM rubber/ carbon filler	Filled elastomer	1.07
SAA-6	A	FM5858	SS-2381 lo-carbon	8HS	HITCO Structures	Staple rayon (F014 resin)	Carbon	1.39
	B	EPDM/Navord XWS 15400 spec	--	--	U.S. Polymeric, Inc.	EPDM rubber/ silica fiber	Filled elastomer	1.06

[a]Section refers to the throat support insulator, and section B refers to the nozzle shell insulator.

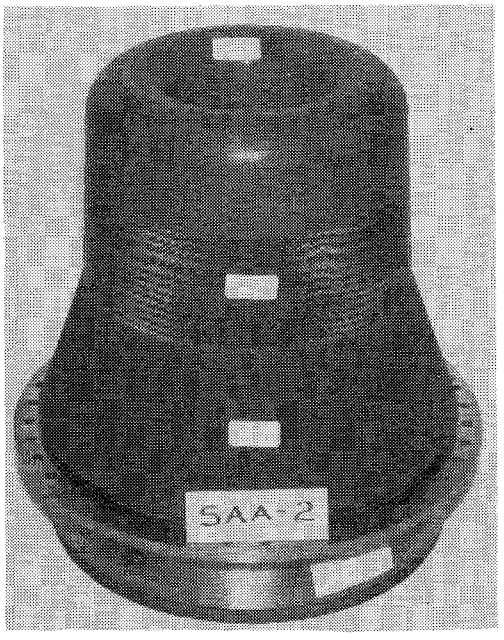

Fig. 3 Typical nozzle assembly—side view.

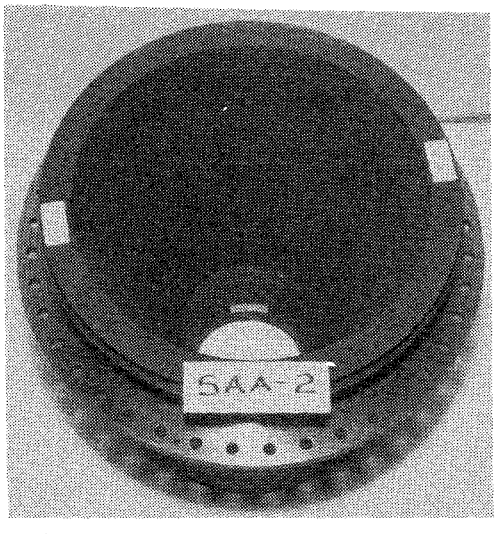

Fig. 4 Typical nozzle assembly—exit cone view.

by the hand layup method and cured on the shell. The nose, throat, and exit cone components were indexed 90 deg on the support shell to assure that material interface joints were not aligned in the axial direction of adjacent components.

Figures 3 and 4 are pretest photographs of a typical completed nozzle assembly showing the nozzle inlet and exit cone, respectively.

Test Configuration, Char Motor

Figure 5 is a cross-sectional view of the Jet Propulsion Laboratory's (JPL) 48-in. diam char motor.[1] This heavy duty test motor was selected because it has the capability to simulate the first portion of the Shuttle SRM chamber pressure-burn time conditions with a reasonable nozzle throat diameter. Figure 6 compares the operating conditions accomplished with the char motor to a typical SRM trace. The motor is mounted on a trailer so that it can be assembled away from the test stand, then brought to the test area, bolted down, and fired. Figure 7 is a pretest photograph of the motor bolted down and ready to fire. Chamber pressure and thermocouple data were recorded for all the tests. A headend carbon dioxide (CO_2) quench system was used to minimize post-test heat soak degradation. A bag containing 0.661 lb of

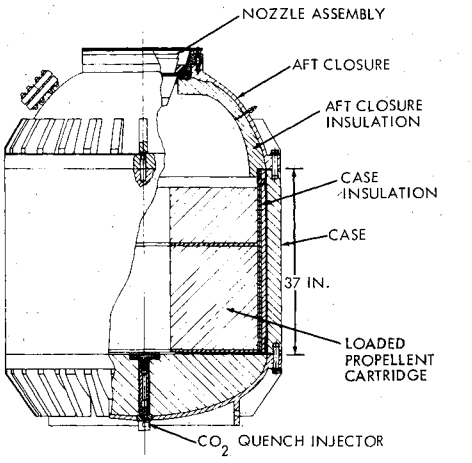

EXPANSION RATIO	8:1
THROAT DIAMETER, IN.	4,000
OVERALL LENGTH OF MOTOR, IN.	76
INSIDE DIAMETER OF CASE, IN.	49.5

Fig. 5 JPL 48-in. char motor cross-sectional view.

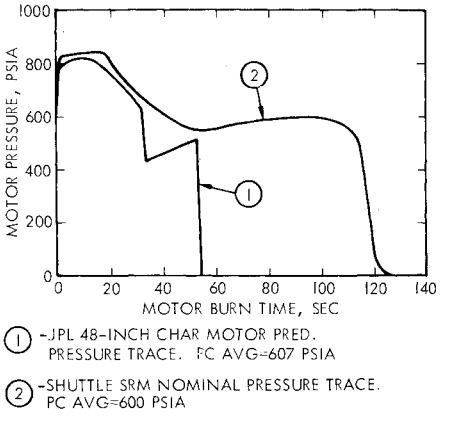

Fig. 6 Comparison of 48-in. char motor and Shuttle booster chamber pressure.

2D and 0.001 lb of 2R boron pellets‡ and two S-89 squibs§ served as the igniter. The propellant is an 86% solids loaded polybutadiene acrylic acid acrylonitrile (PBAN) propellant with 16% aluminum which, except for burn rate modification, is identical to the Shuttle SRM baseline propellant. The propellant formulation and properties are presented in Table 5. The propellant grain design is shown in Fig. 8. Approximately 2100 lb of the SRM-type propellant is cast into an insulated cartridge sleeve. Next, a 0.5-in. thick restrictor is positioned on top of the first casting and approximately 1100 lb of the same propellant is cast to complete the 3200 lb grain. A burn rate of 0.370 in./s was selected as the best based on the anticipated nozzle performance. Verification that the desired burn rate was achieved was accomplished by small (5 lb) motor tests.

Test Results

Ballistic Test Results

The propellant formulation, see Table 5, was formulated to match the Shuttle SRM baseline propellant system except for three modifications. There was an adjustment in the burn-rate catalyst to provide 0.370 in./s at 750 psia; a bimodal (70/30)

‡These pellets are products of M.B. Associates, East Camden, Ark. The R and D designate the pellet diameter.

§These are black powder squibs and are produced by E.I. DuPont de Nemours & Co., Inc.

blend of unground-to-ground oxidizer instead of a trimodal blend; and a plasticizer was used for ease of processing. The propellant was bonded directly to the rubber insulation without the use of a liner system. The propellant properties obtained (Table 5) are shown both as the range (minimum and maximum) and the average of that range, based on the number of mixes. There were a total of 12 batches mixed and cast (six of each size) for testing six nozzles. No attempt was made to adjust the formulation so that the propellant properties would exactly match the SRM propellant properties. That was beyond the scope of this test program. The low value shown for S_m occurred for the last two motors loaded and was due to a new lot of PBAN being used. This new lot was not completely categorized for this program for the reason mentioned earlier, and no attempt was made to adjust the formulation since the values obtained were not detrimental.

Table 6 presents the motor's ballistic characteristics for the six nozzle tests. Figure 9 shows a pressure-time comparison of the nozzles tested. Also shown are pressure-time predictions based on 0, 2.5, 5, 7.5, and 10 mil/s erosion rates. The program was originally planned to test the nozzles at the same average chamber pressure at the SRM, about 600 psia, and a burn time of 50 s or more, therefore, the propellant grain was designed on that assumption. Early in the program, it was decided to test the nozzles at an average chamber pressure of about 750 psia. Rather than change the grain design or close down the nozzle throat, it was decided to adjust the burn rate to provide 0.370 in./s at 750 psia.

Fig. 7 Pretest view of JPL 48-in. char motor.

Nozzle Test Results

The nozzles were inspected and measured prior to testing with respect to concentricity to the nozzle centerline every 45 deg circumferentially at several axial locations on the inner and outer diameter of the assembly. The same measurements were taken after the test. The nozzles were then sectioned and post-fired char depths were measured. Figures 10 and 11 are post-test views of nozzle S/N SAA-2 of the inlet and exit cone, respectively. They can be compared to Figs. 3 and 4 which are pretest views of the same nozzle. Note in Fig. 10 that some

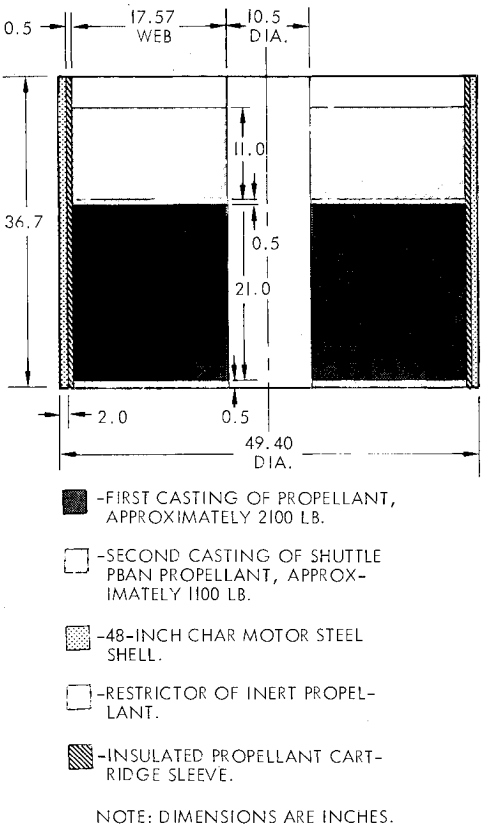

Fig. 8 Char motor propellant grain configuration.

Table 5 Propellant formulation and properties

Propellant ingredients	Weight, %	Weight 1st cast	Weight 2nd cast
Ammonium perchlorate (AP), ung 200 μ	48.95	1076.90	587.40
Ammonium perchlorate (AP), grd 13 μ	21.00	462.00	252.00
Aluminum (Al), 1230	16.00	352.00	192.00
Iron oxide (Fe_2O_3)	0.05	1.10	0.60
Polybutadiene-acrylic acid-acrylonitrile (PBAN)	11.07	243.54	132.84
Dioctyl adipate (DOA)	1.40	30.80	16.80
Epoxy curing agent, DER-331	1.53	33.66	18.36
Batch size	100.00	2200.00	1200.00

Propellant properties

Physical property measured	Range	Average
End of mix viscosity, kps	7.5-15.5	10.6
End of cast viscosity, kps	10.7-17.7	14.6
Density, lb/in.^{3}	0.0639-0.0641	0.0640
Maximum tensile strength, S_m, psi	45.7-98.6	78.5
Elongation at maximum load, E_m, %	28.9-36.6	32.6
Tensile strength at rupture, S_r, psi	44.5-97.2	75.5
Elongation at rupture, E_r, %	31.7-44.5	38.4
Shore 'A' hardness	40 -57	51.8

Table 6 JPL char motor ballistic test results

Motor characteristics	SAA-1	SAA-2	SAA-3	SAA-4[a]	SAA-5	SAA-6
Propellant temperature, °F	77	77	77	77	77	77
Total burn time, s	49.24	49.66	45.78	39.00	48.83	47.25
Web burn time, s	47.45	45.67	43.59	39.00	45.63	45.12
Average chamber pressure, psia	732	785	795	Not avail.	823	782
Maximum chamber pressure, psia	938	941	1034	882	937	995
Pretest throat diameter, in.	3.997	4.000	4.001	4.008	3.999	3.997
Post-test throat diameter, in.	4.639	4.491	4.703	Not avail.	5.150	4.993
Burn rate at average chamber pressure, in./s	0.370	0.378	0.401	Not avail.	0.393	0.340
Propellant weight, lb	3200	3200	3200	3200	3200	3200

[a] Nozzle S/N SAA-4 started failing after 34.04 s burn time. Throat and were cone exit ejected at approximately 39 s.

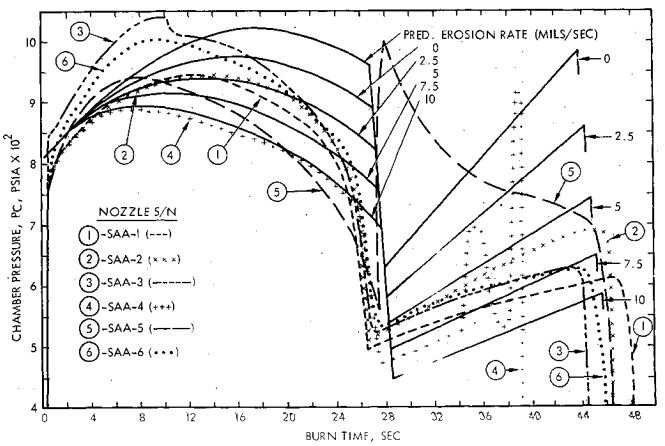

Fig. 9 Pressure-time comparison of SAA nozzle tests.

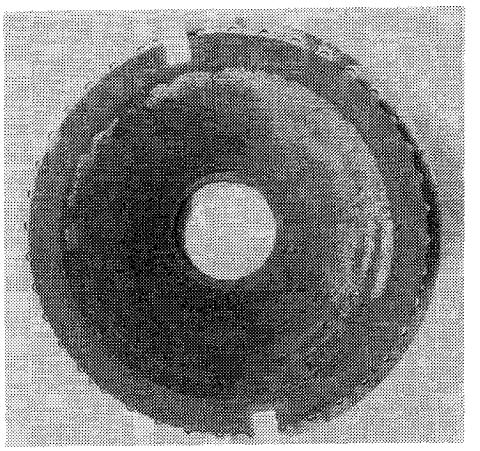

Fig. 11 Post-test exit cone view of SAA-2 nozzle assembly.

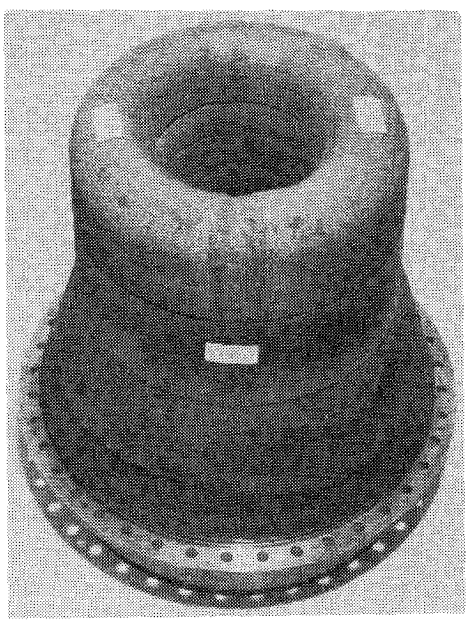

Fig. 10 Post-test inlet view of SAA-2 nozzle assembly.

gouging occurred between the overlap joints on the nose cap. Normal post-test delaminations also occurred. Note in Fig. 11 that the MX4940 exit cone material has a smooth surface while the K421 shows several minor delaminations. In contrast, nozzle S/N SAA-3 had minimal gouging in the nose cap, but severe delaminations. Also, the throat support insulator had cracked through several layers of tape and across the whole width of the tape. It then lifted up from the surface. There were some splits in the rubber insulator of the nozzle shell.

Erosion and Char Results

All the post-test nozzle inspection data that was obtained is summarized and presented in Table 7. Shown is the average radial erosion rate and the char rate for each ablative component tested to date. Also presented are remarks as to the condition of the nozzle, as determined visually, for each component.

All nozzles were successfully tested except for SAA-4. Figure 9 shows that it was eroding at about 11 mil/s until about 34 s into the test when something partially blocked the throat, cleared, and then completely blocked the throat. The throat and exit cone components were then ejected at about 39 s. A complete ring of part of the nose cap was found in the bottom of the motor after the test. It is believed that part of the nose cap delaminated completely by causing a partial flow blockage, and, subsequently, nearly complete blockage of the throat, thus causing the failure. However, sufficient data was obtained, based on Fig. 9, to show that the throat components were eroding at a much higher rate than the other nozzles tested. Also, Fig. 9 shows that nozzles SAA-1 and SAA-2 matched the 5 mil/s prediction for about 16 s and 21 s, respectively. The calculated average throat erosion rates shown in Table 7 agree with the pressure trace on Fig. 9. Nozzles SAA-3 and SAA-6 pressure traces indicated that the throats swelled initially and then began eroding rather quickly, resulting in average throat erosion rates of about 5.5 and 6.5 mil/s (see Table 7). Table 7 shows that some of the exit cone and throat support insulators (component numbers 3 and 4, respectively) swelled minimal amounts during the firing. These are indicated by a minus sign in front of the erosion rates.

Table 7 also presents the average char rates measured for each nozzle component tested, except for SAA-4. The highest char rates were experienced in some of the throat components. This was probably due to the fact that a 90-deg-to-centerline ply orientation was used. None of the materials charred through to the steel support structure.

Table 7 Nozzle test results

S/N[a]	Nozzle Part	Sect.	Material code	Precursor	Avg. radial erosion rate, mils/sec	Avg. char rate, mils/sec	Remarks
SAA-1	Nose cap	A	FM5749	Cont. pitch	6.96	18.8	Both material surfaces very smooth. No structural failures evident.
		B	FM5748	Staple PAN	4.40	10.6	
	Throat	A	FM5749	Cont. pitch	4.80	12.4	Some gouging occurred. Minimal delaminations in both materials.
		B	FM5748	Staple PAN	5.80	13.2	
	Exit cone	A	FM5055[b]	Cont. rayon	-0.70[c]	6.5	Both material surfaces very smooth. No shingling, minimal delaminations (not measurable).
		B	FM5829	Staple rayon	-0.30	6.9	
	Insulators	Throat support	FM5829	Staple rayon	See remarks	9.3	One layer of FM5829 cracked across width of tape and lifted off surface. Rubber eroded away, no damage.
		Nozzle shell	JPL-HTPB rubber	Filled with microballoons	Eroded away	-	
SAA-2	Nose cap	A	K408P	Cont. pitch	1.60	6.24	Both material surfaces very smooth. Minimal delaminations, no structural failures.
		B	K411	Staple PAN	2.18	11.28	
	Throat	A	K408P	Cont. pitch	5.23	10.10	Both sections smooth, no severe delaminations, no structural failures.
		B	K411	Staple PAN	2.53	8.46	
	Exit cone	A	MX4940	Staple rayon	-1.57	6.24	MX4940 surface very smooth, no delaminations. K421 surface was smooth, several delaminations.
		B	K421	Staple PAN	-1.18	7.65	
	Insulators	Throat support	MX4961	Cont. PAN	-0.15	6.44	Both material surfaces very smooth. No cracks, delaminations, or structural failures evident.
		Nozzle shell	Flexwrap 1046B	EPDM rubber	1.40	0.00	
SAA-3	Nose cap	A	K418	Cont. pitch	1.18	No char	Surfaces were smooth, but each had severe delaminations on the reverse flow side.
		B	K414	Staple PAN	5.10	No char	
	Throat	A	K418	Cont. pitch	3.83	9.61	Some gouging in both materials, small number of delaminations, no structural failure.
		B	K414	Staple PAN	7.27	3.06	
	Exit cone	A	K425	Staple PAN	-0.50	7.43	K425 had rough surface, shingling and delaminations, poor structurally. MX4940 had smooth surface, few delaminations.
		B	MX4940	Staple rayon	-0.13	12.50	
	Insulators	Throat support	K432	Staple rayon	See remarks	8.30	K432 had delaminations and cracks across tape width.
		Nozzle shell	Flexwrap 1061B	SBR elastomer	-1.95	8.52	SBR had fairly smooth surface, some axial splits.
SAA-5	Nose cap	d	FM5878	Cont. PAN	Erosion to severe to measure	Same as erosion	Material completely eroded away over 20° arc, severe cracking and delaminating, radial splits.
	Throat	A	MX4964	Cont. pitch	7.30	8.16	Both materials had severe erosion and gouging. Both sections were on the verge of failure.
		B	FM5878	Cont. PAN	16.30	6.76	
	Exit cone	A	MX4960	Cont. PAN	0.85	5.51	Both materials had smooth surfaces. Some channeling due to throat erosion. No delaminations.
		B	MX4961	Cont. PAN	1.40	5.60	
	Insulators	Throat support	FM5856	Staple PAN	0.10	6.81	Both surfaces were smooth, no cracking, delaminations, or spalling.
		Nozzle shell	2066P	EPDM rubber	7.70	0.00	
SAA-6	Nose cap	A	FM5750	Cont. pitch	2.44	9.52	Both material surfaces were smooth with only small delaminations. No structural failures.
		B	FM5064	Cont. rayon	4.50	5.08	
	Throat	A	FM5750	Cont. pitch	3.53	6.77	Both materials had very rough surfaces. Deep gouge in ply overlap region. No other structural failures.
		B	FM5857	Staple PAN	9.53	6.35	
	Exit cone	A	FM5855	Cont. rayon	-0.30	8.69	Both material surfaces were smooth. Only small delaminations. No structural failures.
		B	FM5746	Staple rayon	0.63	7.20	
	Insulators	Throat support	FM5858	Staple rayon	-0.60	6.98	Both material surfaces were smooth. FM5858 had some cross-hatching. EPDM rubber broke during char measurement.
		Nozzle shell	XWS15400	EPDM rubber	-0.40	-	

[a]SAA-4 throat and exit cone were ejected after 39 sec burn time. No measurements taken.
[b]Shuttle nozzle qualified baseline material. [c]Minus sign indicates material swelled.
[d]Nose cap was a ring of one continuous material, no ply overlaps.

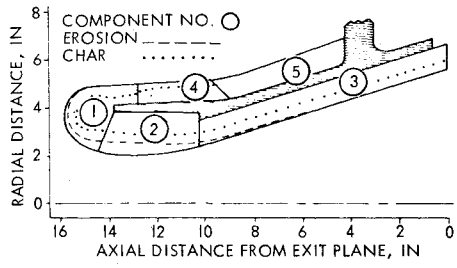

Fig. 12 Typical nozzle erosion and char profile.

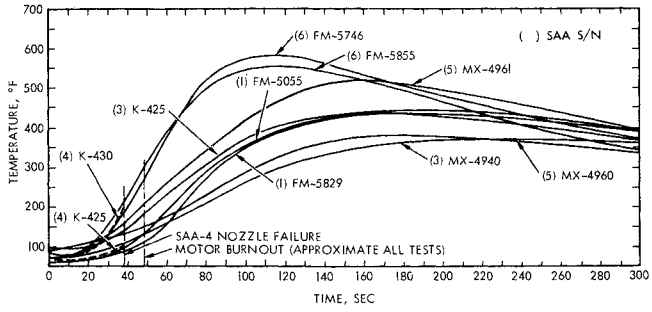

Fig. 13 Subsurface temperatures in SAA exit cones (0.50 in. below surface).

Erosion and char profiles were plotted for each nozzle tested, except for SAA-4. These profiles were plotted every 40 deg circumferentially around the nozzle. A typical erosion and char profile is shown in Fig. 12.

Thermocouple Results

Thermocouples were installed in the exit cone components in order to obtain char rate data. There were a total of eight thermocouples mounted in the same circumferential location through the nozzle steel shell. The thermocouples were placed at 45-deg intervals with the tips alternatively embedded at 0.250 and 0.500 in. from the flame side of the exit cone materials. There were a total of four thermocouples (two at each depth) in each material. The data obtained from all the tests are summarized in Figs. 13 and 14 for the 0.500- and 0.250-in. depths in the form of temperature vs time.

The highest temperature variation was exhibited by a continuous rayon material (FM 5746) followed by two staple materials (rayon and PAN). A continuous pitch material (K 430 of SAA-4) closely followed the staple materials until it was expelled from the nozzle.

Related Test Data

In 1979 NASA Marshall Space Flight Center (MSFC) with the support of the Air Force Rocket Propulsion Laboratory (AFRPL) sponsored two 2.5-in. throat diam nozzle tests that incorporated the Shuttle nozzle continuous rayon carbon phenolic ablative material. The nozzles were identical except the rayon fabric precursor was manufactured by Food Machinery and Chemical Corp. (FMC) for one test and ENKA for the other. They were tested on the Air Force HIPPO test motor using Shuttle PBAN propellant for both firings.[3]

In July 1977 NASA MSFC, with AFRPL support, sponsored a 7-in. throat diam subscale nozzle test. The nozzle configuration was similar to the Shuttle nozzle and was tested on the AFRPL 84-in. char motor using an 8275 lb cylindrical perforated Shuttle PBAN propellant grain.[3]

Table 8 presents the more notable test results for the three motor firings and a detailed discussion is presented in Ref. 3. Figure 15 presents the predicted throat diameter scaling affect on erosion rate using the simplified Bartz equation[4]:

$$ER = MR\ (P_c/P_{cm})0.8\ (D_{tm}/D_t) \qquad (1)$$

Table 8 Related test results

Parameter	2.5 in. throat	7.0 in.
Maximum chamber pressure, psia	825	785
Average chamber pressure, psia	650	650
Motor burn time, s	30	50
Throat erosion rate, mil/s	7.7,[a] 8.4[b]	11.5

[a] FMC material. [b] ENKA material.

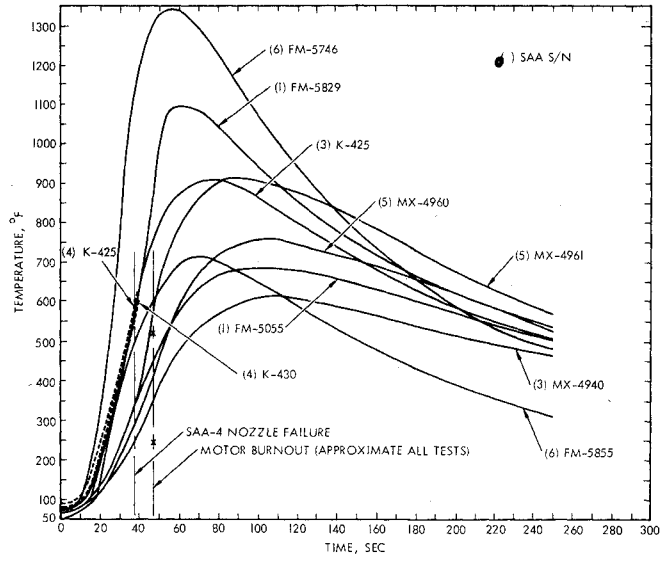

Fig. 14 Subsurface temperatures in SAA exit cones (0.25 in. below surface).

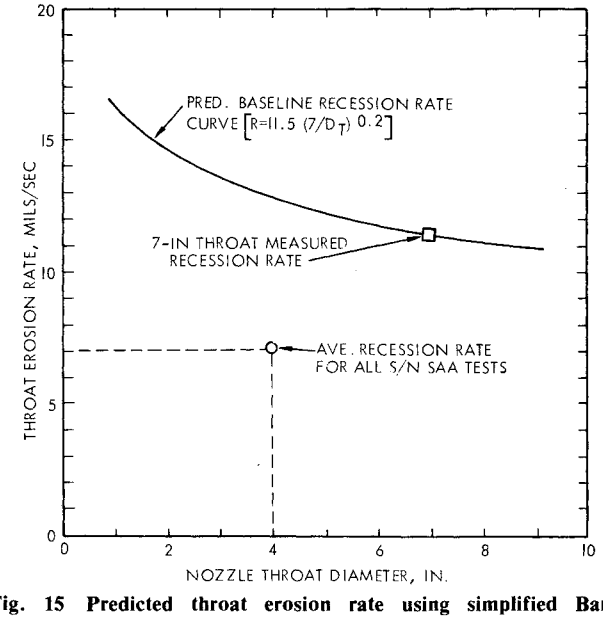

Fig. 15 Predicted throat erosion rate using simplified Bartz equation.

where ER is the erosion rate (mil/s); MR the measured erosion rate (mil/s); P_c the test motor average chamber pressure (psia); P_{cm} the baseline measured motor average chamber pressure (psia); D_t the test nozzle throat diameter (in.); and D_{tm} the baseline motor nozzle throat diameter (in.).

The predicted variation shown in Fig. 15 is based on using the 7-in. test results (Table 8) as the baseline measured data. Therefore, using a baseline erosion rate of 11.5 mil/s, and assuming that the test motor average chamber pressure is the same as the baseline motor, the 4-in. throat is predicted to have an erosion rate of

$$ER = 11.5\ (7.0/4.0)^{0.2}$$
$$= 12.9 \text{ mil/s}$$

This predicted variation shows that the throat erosion rate should increase with decreasing throat diameter if test conditions are constant (nozzle design, propellant type, and grain shape). The submerged 7-in. throat test was used as the baseline reference since the 4-in. throat nozzle design was based on this test and the same propellant system was used for both tests. The 2.5-in. throat test results (Table 8) were not used since this nozzle design was not submerged into the motor. Accordingly, performance of the ablative materials tested was judged based on these test data and the simplified Bartz Eq. (1) above. Therefore, it would be predicted that the erosion rate for the 4-in. throat nozzle (using the average chamber pressure of 783 psia for the five tests) would be

$$\begin{aligned} ER &= 11.5\,(783/650)^{0.8}(7.0/4.0)^{0.2} \\ &= 14.9 \text{ mil/s} \end{aligned}$$

This calculated erosion rate is only 15% higher than the baseline rate curve at the 4-in. throat diam point which is within acceptable limits for this type of data.

Conclusions

Five successful tests were achieved which demonstrated the exceptional performance of the new pitch and PAN ablative materials. Three Fiberite Corp. and three U.S. Polymeric Chemicals, Inc. ablatives utilizing staple PAN and continuous pitch precursors achieved outstanding erosion and char performance. These six materials exhibited throat erosion rates in the 2.5 to 5.8 mil/s range where 9 to 10 mil/s would normally be achieved with the current baseline continuous rayon precursor ablative under similar operating conditions. The average erosion rate for all the tests was 7.01 mil/s and is plotted in Fig. 15 for comparison with the predicted baseline. On the average these ablatives were almost 50% better than predicted. The Fiberite K411 staple PAN was the best candidate in the throat region (2.5 mil/s). Excellent nose erosion performance was also demonstrated. A range of 1.1 to 7.0 mil/s for these same six materials was observed where 10 to 15 mil/s would be expected for the baseline continuous rayon. The Fiberite K418 continuous pitch was the best performing ablative (1.1 mil/s erosion rate) in the nose region.

Acknowledgments

The authors wish to express their thanks to the Fiberite Corp., U.S. Polymeric Chemicals, Inc., HITCO Materials Division, subsidiary of ARMCO, and American Automated Engineering, Inc., for their support in providing the materials and fabrication skills and their excellent cooperation in this effort.

References

[1] Parks, E.G. Jr., "Large Booster Nozzle Reuse Study, Phases II and III," TRW, Cleveland, Ohio, ER-7070-29, Sept. 1969.

[2] Thirkill, J., "Solid Rocket Motor for the Space Shuttle Booster," AIAA Paper 75-1170, Sept. 1975.

[3] Arnold, J., Dodson J., and Lamb, B., "Subscale Solid Motor Tests (Phase IV) and Nozzle Materials Screening and Thermal Characterization (Phase V)," NASA CR-161254, June 1979.

[4] Bartz, D.R., "A Simple Equation for Rapid Estimation of Rocket Nozzle Convective Heat Transfer Coefficients," *Jet Propulsion Laboratory*, Vol. 27, No. 1, Jan. 1957.